Hindawi
International Journal of Chemical Engineering
Volume 2022, Article ID 1374993, 15 pages
https://doi.org/10.1155/2022/1374993

Research Article

Electrochemical Denitrification of Synthetic Aqueous Solution and Actual Contaminated Well Water: RSM Modeling, Kinetic Study, Monte Carlo Optimization, and Sensitivity Analysis

Fahimeh Shamseali,[1] **Farzaneh Mohammadi**,[2,3] **Hamidreza Pourzamani**,[2,3] **and Mahsa Janati**[4]

[1]*Student Research Committee, School of Health, Isfahan University of Medical Sciences, Isfahan, Iran*
[2]*Department of Environmental Health Engineering, School of Health, Isfahan University of Medical Sciences, Isfahan, Iran*
[3]*Environment Research Center, Research Institute for Primordial Prevention of Non-Communicable Disease, Isfahan University of Medical Sciences, Isfahan, Iran*
[4]*Lakehead University, Thunder Bay, Canada*

Correspondence should be addressed to Farzaneh Mohammadi; fm_1363@hlth.mui.ac.ir

Received 19 July 2022; Accepted 10 October 2022; Published 28 October 2022

Academic Editor: Sébastien Déon

The process of electrochemical denitrification is applied with the aim of converting nitrate (NO_3^-) to N_2 gas by reducing nitrate and oxidizing by-products such as ammonia (NH_4^+). In this study, Ti/RuO_2 and graphite were used as anode and cathode electrodes, respectively, to treat synthetic aqueous solutions containing different concentrations of nitrate ions. Nitrate initial concentration (2.75–55 mg NO_3-N/lit), voltage (2.5–30 V), pH (3–13), electrode distance (ED = 0.5–3.5 cm), and reaction time (10–180 min) were the main studied operating parameters for the electrochemical denitrification (ECD) reactor. The experiments were designed using the central composite design (CCD) method. The experimental results were modeled with the response surface methodology (RSM) technique. Scanning electron microscope (SEM), X-ray diffraction analyzer (XRD), and Fourier transform infrared spectroscopy (FTIR) characterized electrodes were performed before and after all experiments. Optimization and sensitivity analysis was performed using the Monte Carlo simulation (MSC) approach. The energy consumption and current efficiency were calculated for the ECD reactor. Kinetic models of zero, first, and second order were evaluated, and the second-order model was selected as the best kinetic model. Also, the effect of adding monovalent, divalent salts, and organic compounds to the process was evaluated. Finally, three nitrate-contaminated water wells were selected near agricultural lands as real samples and investigated the performance of the ECD process on the samples. The performance of the ECD reactor for the real samples showed some decrease compared to the synthetic samples.

1. Introduction

All living organisms need nitrogen in some way, but some nitrogenous compounds can pose chemical hazards to aquatic and nonaquatic organisms. There are three important forms of nitrogen in aquatic environments, which are ammonium ion (NH_4^+), nitrite (NO_2^-), and nitrate (NO_3^-) [1]. Groundwater is predominantly exposed to nitrate contamination around agricultural areas [2]. In addition, surface water to which effluents are discharged is highly susceptible to nitrate contamination [3, 4]. High concentrations of nitrate cause methemoglobinemia (Blue Baby Syndrome) and gastrointestinal cancers [5]. For these reasons, the World Health Organization (WHO) has set 50 mg/lit as the maximum permissible level for (NO_3^-) in drinking water. Hence, it is necessary to reduce NO_3^- concentration in water resources [6].

There are a variety of physicochemical processes for nitrate removal, including chemical precipitation, distillation, reverse osmosis, electrodialysis, ion exchange, and

biological denitrification [7]. Each of these processes has its advantages and disadvantages [8]. For instance, ion exchange methods are economical for removing NO_3^- but they are not specific for the ions of interest and yield a great deal of concentrated brine containing sulfate, chloride, and NO_3^- that need to be disposed of separately [9, 10]. Also, using of metallic iron and aluminum powder has been investigated to reduce NO_3^- in water; the strong dependence of the process on pH is its disadvantage [11]. In the biological denitrification process, NO_3^- is selectively removed with little waste. Nevertheless, carbon sources must be carefully monitored to ensure this process succeeds. NO_3^- removal present in the current processes has various limitations and is especially unsuitable for small communities [8].

According to the previous studies, electrochemical oxidation (EO) is a high-efficiency alternative to the above-mentioned processes treating nitrate-contaminated water. It is also fast and easy to operate [12]. Many types of electrodes have been investigated for electrochemical treatment, such as TiO_2, Ti, Fe, PbO_2/Ti, SnO_2/Ti, and aluminum [13–15]. Cathode metals and their alloys, including graphite [16], Ru [17], Cu [18], BDD [19], Ir [17], Pt/Cu [20], Zn [21], CO_3O_4 [12], Ni [22], Pd [23], Pt [17], Fe [24] have been reported for EO processes. Graphite is one of the promising cathodes among them due to its high efficiency, cost-effectiveness, nontoxic, and corrosion resistance in aqueous solutions. The Ti/RuO_2 electrode is one of the promising electrodes for the electrochemical reduction of nitrate, Ti is a good substrate for the electrodeposition of metal oxides due to its chemical stability, mechanical strength, surface area, corrosion resistance, wide electrochemical potential window, and low cost [25–27]. Ru has the highest activity toward nitrate reduction [28]. Thus, graphite as the cathode and Ti/RuO_2 as the anode could be potentially a very promising mixture for highly effective and economical EO processes than other combinations [3].

Modeling and optimizing of the chemical processes input parameters to achieve the highest efficiency is a challenging task. Recently, response surface method (RSM) has been used to model and find interactions between independent input parameters in chemical processes. RSM is a statistical technique based on multivariate regression. Experiment design techniques, such as Box–Behnken and Central Compound Design (CCD), are also used to reduce the number of experiments while measuring important points in the modeling. The CCD is an integral part of response surface mythology. The biggest advantage of this type of optimization model is, it is more accurate, and no need for a three-level factorial experiment for building a second-order quadratic model [29].

In this study, nitrate was removed through the ECD process, and the kinetics of the process was also investigated. Also, the results were modeled using response surface methodology (RSM). Optimization and sensitivity analysis was performed through Monte Carlo simulation. The five quantitative variables of nitrate concentration, voltage, pH, electrode distance, and reaction time were investigated. Initial experiments were performed on synthetic samples. Then, after determining the optimal conditions, the efficiency of the process was evaluated on actual well water samples contaminated with nitrates.

2. Experimental

2.1. Materials and Reagents. Sodium chloride (NaCl, 99.5%), sodium nitrate ($NaNO_3$, 98%), zinc sulfate heptahydrate ($ZnSO4 * 7H_2O$), and glucose monohydrate ($C_6H_{12}O_6 * H_2O$) were obtained from Merck (Darmstadt, Germany). Ti/RuO_2 commercial electrode was prepared from PNPB Co., Ltd., Iran (https://www.pt-catalyst.com/). The graphite electrode was purchased from Azar Electrode Company, Iran. A cellulose acetate (CA) membrane filter was prepared with a pore size of 0.45 μm, 47 mm in diameter (Microlab Scientific Co., Ltd., China). H_2SO_4 and NaOH aqueous solutions (0.1 mol/Lit) were used for pH adjustment. All samples were prepared in double-distilled water.

Hach NitraVer® 5 Nitrate and NitriVer® 3 Nitrite Reagents Powder Pillows were used to measure nitrate and nitrite. The Nessler method measured ammonia (NH_4^+) in aqueous samples. Nessler reagent was prepared with sodium hydroxide (NaOH, 98%, Merck), potassium iodide (KI, 99.5%, Merck), and mercury chloride ($HgCl_2$, 99.5%, Neutron Pharma Chemical Co., Iran).

2.2. Design of Experiments. This study used the central composite design (CCD) method to design the experiments. In the CCD method, each factor has five different levels. The RSM model was implemented using Design-Expert software, version 13.0.9. The actual and coded values of the variables are shown in Table 1 and the suggested experiments using the CCD method are shown in Table 2. The independent variables are initial concentration (mg (NO_3-N)/L), voltage (V), pH, electrode distance (ED) (cm), and time (min) and the response parameter is nitrate removal. In this study, 47 experiments with 5 replication points were required. The main response was nitrate removal, but at the end of each experiment, the concentration of ammonia and nitrite was also measured. In addition, the current density (mA/cm^2) was recorded at the beginning and end of each experiment.

2.3. EC Reactor. A plexiglass box (10 cm W × 10 cm L × 20 cm H) with a volume of 2000 mL was used as a reactor (Figure 1). A Ti/RuO_2 (8×7 cm^2; 1 mm thickness) sheet was used as the anodic electrode and carbon graphite (8×7 cm^2; 8 mm thickness) sheet was used as the cathodic electrode, with an effective electrode surface area of 84 cm^2. The two electrodes were placed in parallel as described in Figure 1. Then, different distances between them were set up with an insulating rod. Electrodes were connected to a D.C power supply (Dangheng, Vietnam, Model: A305D; 0–6 A, 0–30 V) which controlled the voltage and current of the electrolysis. A magnetic stirrer was installed under the reactor at 180 rpm speed to ensure continuous mixing in the solution. The electrodes were placed on two stands at a height of 3 cm from the bottom of the ECD reactor to easily mix the whole solution. Different nitrate concentrations were made using

Table 1: The levels of independent variables.

Factor	Name	Units	Type	Min	Max	Coded low	Coded high
A	Initial concentration	mg N/L	Numeric	2.75	55.0	−1↔2.75	+1↔55
B	Voltage	V	Numeric	2.5	30.0	−1↔2.5	+1↔30
C	pH	—	Numeric	3.0	13.0	−1↔3	+1↔13
D	Electrode distance	Cm	Numeric	0.50	3.50	−1↔0.5	+1↔3.5
E	Time	Min	Numeric	10.0	180.0	−1↔10	+1↔180

Table 2: The proposed experiments using the CCD method.

Run	A: initial concentration (mg N/L)	B: voltage V	C: pH —	D: ED (cm)	E: time (min)	Removal rate
1	2.75	15.0	8	2	90	0.58
2	2.75	15.0	8	2	90	0.60
3	11	7.5	12	1	35	0.62
4	11	7.5	12	3	35	0.53
5	11	22.5	4	1	150	0.52
6	11	7.5	4	1	150	0.51
7	11	7.5	4	1	35	0.48
8	11	22.5	4	3	150	0.42
9	11	7.5	4	3	35	0.39
10	11	22.5	12	3	35	0.57
11	11	22.5	4	1	35	0.50
12	11	7.5	4	3	150	0.38
13	11	22.5	12	1	150	0.73
14	11	22.5	12	3	150	0.63
15	11	7.5	12	3	150	0.56
16	11	22.5	4	3	35	0.45
17	11	7.5	12	1	150	0.66
18	11	22.5	12	1	35	0.66
19	27.5	15.0	8	2	90	0.85
20	27.5	15.0	8	3.5	90	0.79
21	27.5	15.0	8	0.5	90	0.91
22	27.5	30.0	8	2	90	0.97
23	27.5	15.0	8	2	180	0.86
24	27.5	2.5	8	2	90	0.94
25	27.5	15.0	3	2	90	0.56
26	27.5	15.0	13	2	90	0.71
27	27.5	15.0	8	2	10	0.77
28	27.5	15.0	8	2	90	0.84
29	27.5	15.0	8	2	90	0.90
30	44	22.5	12	3	150	0.69
31	44	22.5	4	1	150	0.66
32	44	7.5	4	3	35	0.54
33	44	7.5	12	1	35	0.74
34	44	22.5	4	3	150	0.57
35	44	22.5	4	1	35	0.66
36	44	7.5	4	1	150	0.67
37	44	22.5	12	3	35	0.65
38	44	7.5	12	3	150	0.65
39	44	22.5	12	1	35	0.74
40	44	22.5	12	1	150	0.74
41	44	7.5	4	1	35	0.68
42	44	22.5	4	3	35	0.58
43	44	7.5	12	3	35	0.64
44	44	7.5	4	3	150	0.53
45	44	7.5	12	1	150	0.72
46	55	15.0	8	2	90	0.68
47	55	15.0	8	2	90	0.72

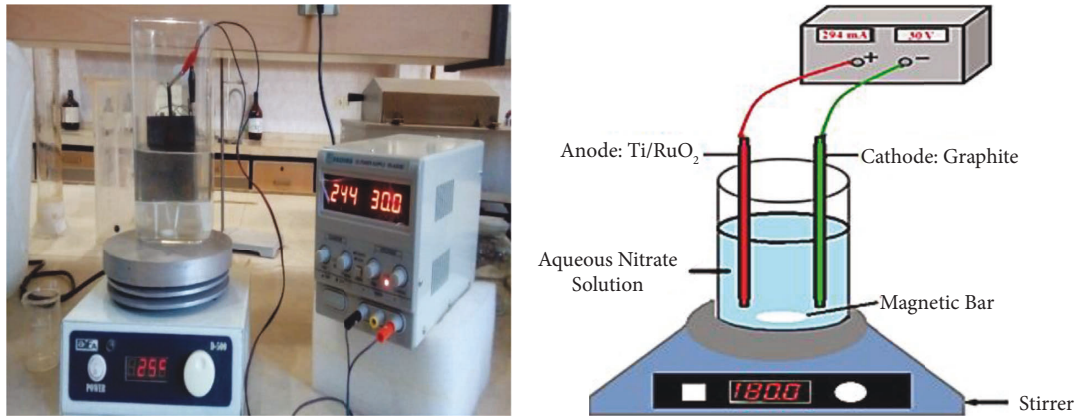

Figure 1: (a) Laboratory scale ECD reactor. (b) Schematic ECD reactor.

sodium nitrate and distilled water in a volume of 800 ml. All of the batch experiments conducted at room temperature of $25 \pm 2^{\circ}C$.

2.4. Degradation Pathway and Mass Balance Study. Batch treatment of nitrate-contaminated solutions by the ECD method involves two basic mechanisms. In one case, nitrate is directly reduced to N_2 by cathodic reduction with different by-products, in the other, nitrate is indirectly reduced to N_2 during water electrolysis at the cathode, By-products such as nitrite and ammonia are indirectly oxidized by free radicals generated in-situ, such as hydroxyl radicals. Adsorption of nitrate on the surface of the cathode induces direct reduction of nitrate into N_2, NH_3, and other by-products. The main chemical reactions that occur on the cathode surface are mentioned as follows [3, 30]:

$$NO_3^- + 3H_2O + 5e^- \longrightarrow \frac{1}{2}N_2 + 6OH^-, \quad (1)$$

$$NO_3^- + 6H_2O + 8e^- \longrightarrow NH_3 + 9OH^-, \quad (2)$$

$$NH_3 + 3OH^- \longrightarrow \frac{1}{2}N_2 + 3H_2O + 3e^-. \quad (3)$$

The nitrite electrogenerated is an intermediary by-product and can be converted into ammonia, nitrogen gaseous, and also nitrate according through the following reactions:

$$NO_2^- + 5H_2O + 6e^- \longrightarrow NH_3 + 7OH^-. \quad (4)$$

$$2NO_2^- + 4H_2O + 6e^- \longrightarrow N_2 + 8OH^-. \quad (5)$$

$$NO_2^- + 2OH^- \longrightarrow NO_3^- + H_2O + 2e^-. \quad (6)$$

According to the studies of Liou et al. [31], Zhao et al. [32], and Babaei [33], and others [3, 34, 35], the intermediate products, such as N_2O, NO, NH_2OH, and NH_2NH_2, were confirmed to be negligible in nitrate reduction process using various advanced oxidation methods. Therefore, in this study, the denitrification rate can be calculated using mass balance based on nitrate, nitrite, and ammonium concentration. The nitrogen concentration was directly reduced to nitrogen gas is calculated from the following equation:

$$TN_i = (NO_3^- - N)_f + (NO_2^- - N)_f + (NH_4^+ - N)_f + (N_2 - N)_f. \quad (7)$$

In the present study in ECD lab experiments,

$$TN_i = (NO_3^- - N)_i, \quad (8)$$

where TN_i, $NO_3^- - N$, $NO_2^- - N$, $NH_4^+ - N$, and $N_2 - N$ are the total nitrogen ($mg{\cdot}N{\cdot}L^{-1}$), nitrate nitrogen concentration ($mg{\cdot}N{\cdot}L^{-1}$), nitrite nitrogen concentration ($mg{\cdot}N{\cdot}L^{-1}$), ammonium nitrogen concentration ($mg{\cdot}N{\cdot}L^{-1}$), and nitrogen gas ($mg{\cdot}N{\cdot}L^{-1}$), respectively. The indices "i" and "f" indicate the values at the beginning and end of the experiments. The following equations were applied for nitrate removal rate and denitrification rate calculation [36].

$$\text{Nitrate removal rate} = \frac{(NO_3^- - N)_i - (NO_3^- - N)_f}{(NO_3^- - N)_i}, \quad (9)$$

$$\text{Denitrification rate} = \frac{(N_2 - N)_f}{(TN)_i}. \quad (10)$$

2.5. Measurement Methods, Instruments, and Electrode Characterization. All analyses were conducted according to standard methods [37]. Before measurement, all solutions were filtered through the cellulose acetate (CA) membrane. The concentration of ammonia was measured by the Nessler method at 420 nm. The concentration of nitrate and nitrite were measured at 500 and 507 nm, respectively, with the Hach DR 5000™ UV-Vis Laboratory Spectrophotometer. Eutech Instruments (CyberScan pH 1500) pH meter was used to check the pH of the solutions. The microstructure and morphology of the electrodes before and after all experiments were carried out by X-ray diffraction (XRD, X′ Pert-MPD, Philips, Netherlands),

scanning electron microscopy (SEM, XL 30 ESEM with EDAX, Philips, Netherlands), and Fourier transform infrared spectroscopy (FTIR, Bruker, Germany), respectively.

2.6. Optimization and Sensitivity Analysis by Monte Carlo Simulation. Monte Carlo simulation (MCS) is a mathematical technique used to estimate the possible outcomes of an uncertain event. An MCS generates a different set of random numbers using the probability distribution of each variable, which has inherent uncertainty, and then recalculates the results in the distribution of the variables. In this study, 10,000 data were produced to reach likely outcomes [38]. RStudio software version 2022.02.2 and Monte Carlo package version 1.06 were applied for MCS calculation. In this method, it is first necessary to determine the statistical distributions for the input parameters. At this time, the fitdistrplus package version 1.1–1.8 in RStudio software was used for distribution fitting. The statistical distributions provided for input variables (initial concentration, voltage, pH, electrode distance, and time) are represented in Table 3. Then, based on the statistical distribution of each parameter, 10,000 data were produced using *R* software. Thereafter, all generated data were placed in the output equation of the RSM model and the nitrate removal rate was calculated. Five points with the highest removal rate in the results were selected and were experimented within the laboratory to select the optimal point.

Finally, the magnitude order of the influence of the input variables on the response variable (nitrate removal) will be determined using the sensitivity analysis approach. The sensitivity analysis was performed using Spearman's rank correlation coefficient technique on MCS data.

2.7. Kinetics Evaluation of the Nitrate Removal Process. The kinetics of nitrate removal by electrochemical denitrification process were analyzed using three kinetic models (zero-order, first-order, and second-order) to find the one that best describes the nitrate removal process. The kinetic equations are shown in the following expressions:

Zero-order kinetic model:

$$\frac{-\Delta\left[\left(NO_3^- - N\right)\right]}{\Delta t} = k. \tag{11}$$

First-order kinetic model:

$$\frac{-\Delta\left[\left(NO_3^- - N\right)\right]}{\Delta t} = k_1\left[\left(NO_3^- - N\right)\right]. \tag{12}$$

Second-order kinetic model:

$$\frac{-\Delta\left[\left(NO_3^- - N\right)\right]}{\Delta t} = k_2\left[\left(NO_3^- - N\right)\right]^2, \tag{13}$$

where k, k_1, and k_2 are the rate constants for zero order ($mg{\cdot}L^{-1}{\cdot}min^{-1}$), first order ($min^{-1}$), and second order ($L{\cdot}mg^{-1}{\cdot}min^{-1}$), respectively. To calculate the kinetic constants, the diagrams of time (min) versus C_t/C_o, $1/(C_t/C_o)$, and (C_t/C_o) were drawn, respectively. Here, C_0 represents the initial nitrate concentration and C_t stands for the nitrate concentration at time t.

2.8. Addition of Inorganic and Organic Compounds in the ECD Process. Sodium chloride (NaCl) and zinc sulfate heptahydrate ($ZnSO_4 * 7H_2O$) as inorganic compounds, and glucose as the organic compound were added to the ECD reactor at concentrations of 1, 10, 100, 1000 ($mg{\cdot}L^{-1}$) at the optimum point. The goal was to evaluate the influence of concentration, class of chemicals (organic and inorganic compounds), and salt capacity (monovalent and divalent ions) on the nitrate removal efficiency.

2.9. Nitrate Removal of Actual Samples by the ECD Reactor. To investigate the performance of the ECD process on actual samples, three nitrate-contaminated drinking water wells were selected around the agricultural lands in Iran. After measuring TDS and nitrate in the samples, the nitrate removal efficiency was evaluated in the ECD reactor under optimal conditions.

3. Result and Discussion

3.1. RSM Model Implementation for ECD Process. The experiments were designed using the CCD method to evaluate nitrate removal in the ECD process. The results of the experiments and the nitrate removal rate can be observed in Table 2. To implement the RSM model, initially, it is necessary to perform analysis of variance (ANOVA) and evaluate the significance of the model and its variables. The ANOVA results for the quadratic RSM model are tabulated in Table 4. *F*-value equal to 136.36 indicates that the quadratic model was the significant model (p value < 0.05) for the experiments. Variables with the p value of less than 0.1 were kept in the model after variable selection. Also, based on the calculated *F*-values for internal variables, pH, electrode distance, initial concentration, and voltage are inferred to have significant influences on the nitrate removal in the ECD process. In contrast, the time can be inferred to be less significant. The Lack-of-fit test was not significant as the p values were greater than 0.05. R^2 and adjusted-R^2 values (0.985, 0.978) imply a major correlation between the predicted and actual data. The predicted R^2 value of 0.963 indicates the suggested model could predict responses well for new experimental observations. The adequate precision for the elimination of nitrate was 49.42. Adequate precision values greater than 4 indicate the adequacy of the model [39, 40].

The final equation in terms of coded factors is as follows:

$$\begin{aligned}\text{Nitrate Removal Rate} = {} & +0.8822 + 0.0614A + 0.0352B + \\ & 0.0765C - 0.0673D + 0.0096E - 0.0195AB - \\ & 0.0408AC - 0.0142AE + 0.0193BD + 0.0134CE - \\ & 0.2353A^2 + 0.0698B^2 - 0.2513C^2 - 0.0345D^2 - 0.0658E^2.\end{aligned} \tag{14}$$

To accurately assess the model performance, diagnostic diagrams were also drawn, which can be seen in Figure 2. Figure 2(a) illustrates the relation between predicted vs. actual values. A model with an R^2 value of 1 will have all data

Table 3: Variables statistical distributions.

Variables	Unit	Distribution
Initial concentration	$mgNO_3$-N/L	Weibull ($\alpha = 1.4422$ $\beta = 31.596$)
Voltage	V	Weibull ($\alpha = 2.0112$ $\beta = 17.131$)
pH	—	Beta ($\alpha 1 = 0.52313$ $\alpha 2 = 0.52313$ $a = 3.0$ $b = 13.0$)
ED	Cm	Uniform ($a = 0.45713$ $b = 3.5429$)
Time	Min	Uniform ($a = 3.329$ $b = 180.5$)

Table 4: ANOVA analysis for RSM modeling.

Source	Sum of squares	Degrees of freedom	Mean square	F-value	p value	
Model	0.9082	15	0.0605	136.36	<0.0001	Significant
A-initial concentration	0.0592	1	0.0592	133.37	<0.0001	
B-voltage	0.0127	1	0.0127	28.67	<0.0001	
C-pH	0.1302	1	0.1302	293.20	<0.0001	
D-electrode distance	0.0713	1	0.0713	160.64	<0.0001	
E-time	0.0015	1	0.0015	3.39	0.0750	
AB	0.0014	1	0.0014	3.24	0.0815	
AC	0.0136	1	0.0136	30.70	<0.0001	
AE	0.0012	1	0.0012	2.67	0.1123	
BD	0.0016	1	0.0016	3.53	0.0696	
CE	0.0017	1	0.0017	3.80	0.0604	
A^2	0.1703	1	0.1703	383.57	<0.0001	
B^2	0.0096	1	0.0096	21.52	<0.0001	
C^2	0.2012	1	0.2012	453.16	<0.0001	
D^2	0.0027	1	0.0027	6.03	0.0199	
E^2	0.0100	1	0.0100	22.42	<0.0001	
Residual	0.0138	31	0.0004			
Lack of fit	0.0105	27	0.0004	0.4780	0.8904	Not significant
Pure error	0.0033	4	0.0008			
Cor total	0.9219	46				
	R^2			0.9851		
	Predicted R^2			0.963		
	Adjusted R^2			0.9778		
	Adeq precision			49.4276		

points on the line. Lower the R^2 value, data points will be farther away from the line. Figure 2(a) indicates that this model looks appropriate, and the data has no noise. The model accuracy was also investigated based on the normal probability plots of the studentized residuals for nitrate removal rate in Figure 2(b). In this figure, if all points fall on the line, the model fits the data well and the error variance is homogeneous.

3.2. Effects of Independent Variables on Nitrate Removal. In the present study, the influence of input variables, including initial concentration (C_0), voltage, pH, electrode distance (ED), and time was investigated on nitrate removal in the ECD process. Using the RSM model, the variation of response variable based on input variables was illustrated in Figure 3. Figure 3(a) shows the interaction of initial concentration and pH versus the nitrate removal rate. It is quite evident that the initial concentration and pH have nonlinear effects on the removal efficiency. The nitrate removal in highly acidic solutions was low (pH = 3); as the solution's pH increased, the efficiency also increased. The highest efficiency occurred in the range close to pH 10 and the initial concentration of 30 ($mg{\cdot}L^{-1}$). Thereafter, the nitrate removal efficiency decreased in highly alkaline solutions (pH 12, 13). Chauhan et al. [3] investigated the denitrification of actual nitrate wastewater by using an electrochemical process and implied at pH 10–12 the maximum removal of nitrate reduction occurred. Miao Li et al. [34] found at low pH (4.0–4.8) the nitrate reduction rate was the lowest and at high pH (9.2–10.1) the nitrate reduction rate was the highest; it is in agreement with our experimental data.

Figures 3(b) and 3(c) show the interactive effects of ED vs. voltage and ED vs. CD (current density), respectively, on nitrate removal efficiency. Nitrate removal increases with decreasing distance from 3 cm to 0.5 cm and increasing voltage from 10 V to 30 V. Other research indicated that the wider the electrode distance, the lower the removal efficiency [41, 42]. Although the current density parameter was not one of the independent parameters in this experiment, with increasing voltage, initial concentration, pH, and decreasing the distance between the electrodes, the current increased, followed by the efficiency increase because of more production of OH radicals during the process (Figure 3(c)) [43–45]. Figure 3(d) shows the interaction of initial concentration and time on nitrate removal. The efficiency

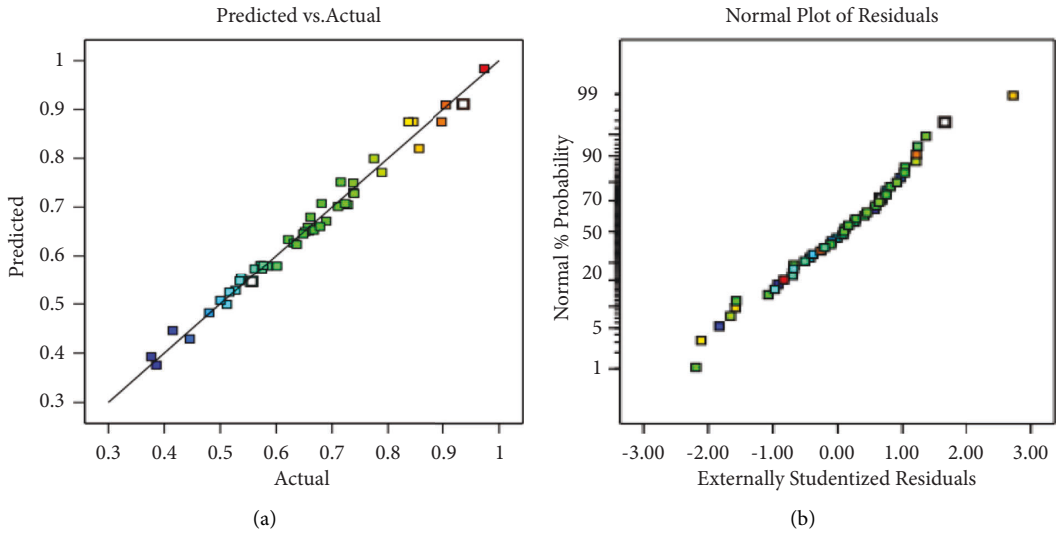

Figure 2: (a) Actual vs. predicted plot and (b) normal % probability vs. studentized residual plot, for nitrate removal rate.

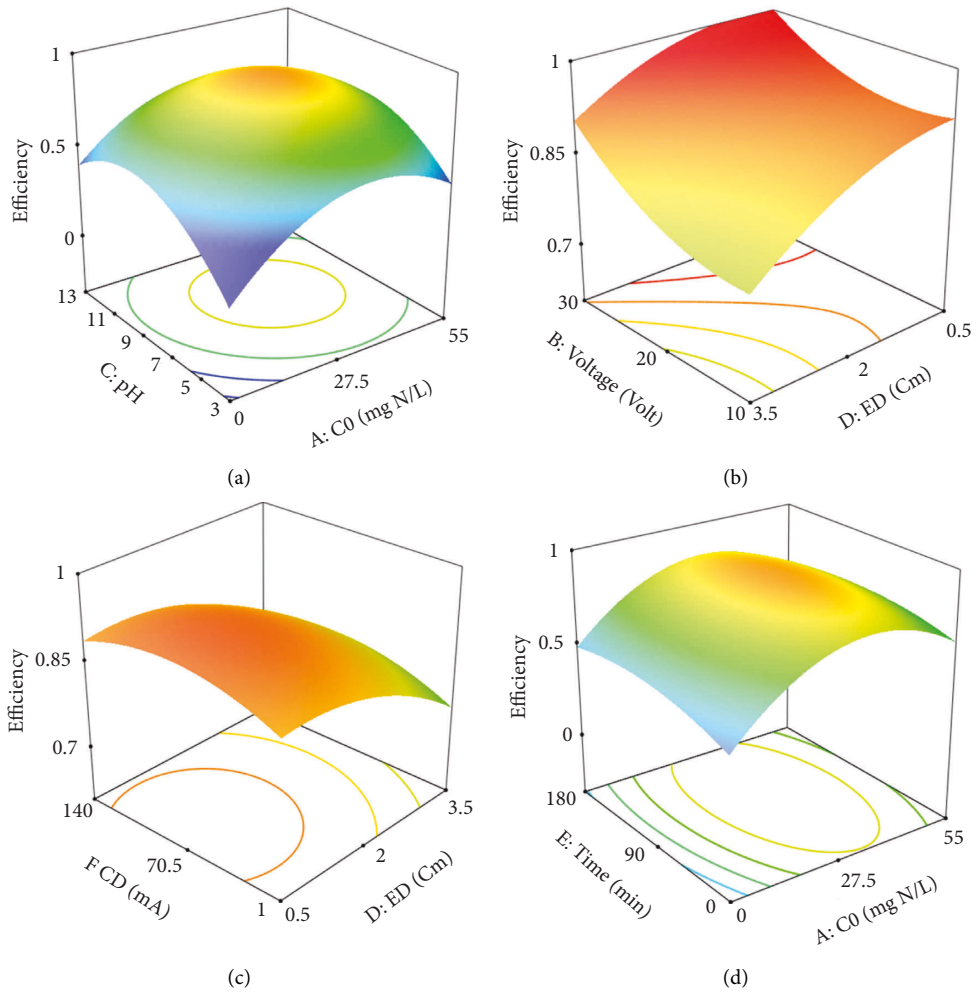

Figure 3: 3D surface plots for nitrate removal efficiency using EO process.

increased with increasing initial concentration to about 30 mg/l. As shown in Figure 3 initial concentrations from 30 to under 55 mg·N/L caused a slightly reduced nitrate removal efficiency, this was also reported by Benekos et al. A change in the time parameter at 90 min resulted in the highest removal efficiency after which no significant change

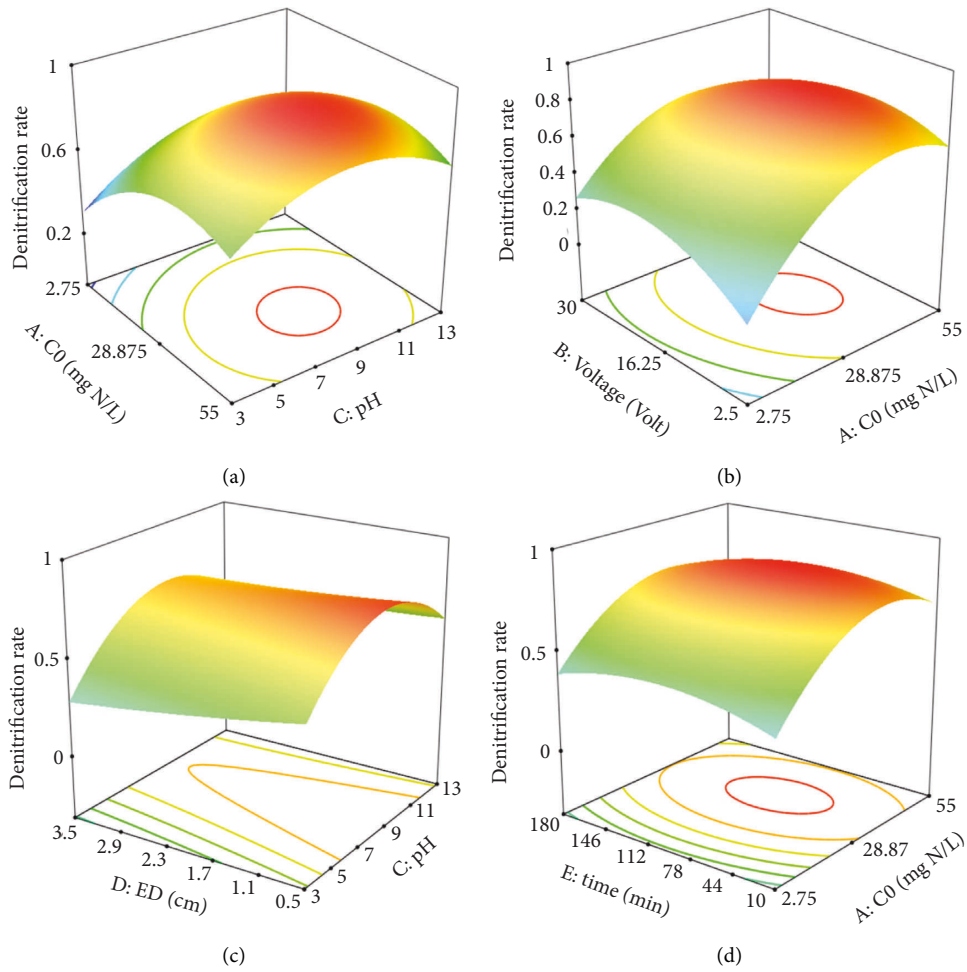

Figure 4: 3D surface plots for denitrification rate.

was observed. Nitrite anions were also present but in small amounts (0.08–0.007 mg NO_2^-N/L), that is, because nitrite is easily converted to ammonia and nitrate by the ECD process. Therefore, we omitted the analysis of nitrite output data such as other similar studies [34].

3.3. Effects of Independent Variables on Denitrification Rate. The interaction of C_0 and pH on denitrification rate was shown in Figure 4(a). The denitrification rate was found to be minimum in the highly acidic environment (pH = 3). As pH increased, the higher denitrification rate was observed up to pH of ≈11. Thereafter, in highly alkaline conditions (pH > 11), the denitrification rate slightly decreased. This is consistent with previous studies [46, 47]. The denitrification was extremely poor at the low C_0 of 2.75 (mg N/L). As shown in Figure 4(b) The interaction of voltage and C_0, the denitrification was extremely poor at the low voltage of 2.5 V, which increased with the increase in C_0 and voltage. The effect of C_0 on denitrification was slightly more prominent than the effect of voltage. The interaction of pH vs. ED and C_0 vs. time on denitrification rate is shown in Figures 4(c) and 4(d), respectively. Changes in electrode distance had the least significant effect on the denitrification rate.

3.4. Effects of Independent Variables on Ammonia Concentration. As shown in response surface plots in Figure 5(a), higher initial nitrate concentrations (C_0) lead to higher NH_4^+-N concentrations. At alkaline pH, the value of NH_4^+-N decreased due to decreasing the solubility of NH_4^+ cations in the liquid phase in alkaline conditions [46]. Whereas at low pH, the EO process produced NH_4^+ [3]. Therefore, the concentration of NH_4^+-N increases with decreasing pH. The effect of voltage is shown in Figure 5(b), the NH_4^+-N concentration diminished with increasing voltage from 2.5 V to 30 V in the EC process. Figure 5(c) shows the interactive effects of ED vs. time. The lowest amount of ammonium ion has been observed at the lowest distance between the electrodes. As the electrode distance increased, the current availability to the anode-cathode was decreased. Therefore, the reaction rate at the anode-cathode reduced, leading to an increase in the concentration of NH_4^+-N (Figure 5(c)) [48]. In 180 minutes, the concentration of NH_4^+-N falls from 2.5 ($mg{\cdot}L^{-1}$) to closer to 0 ($mg{\cdot}L^{-1}$).

3.5. Characterization of Electrode. The FE-SEM analysis was conducted to examine cathode and anode surface morphology (Figure 6(a)). Anode (Ti/RuO_2) was regular with

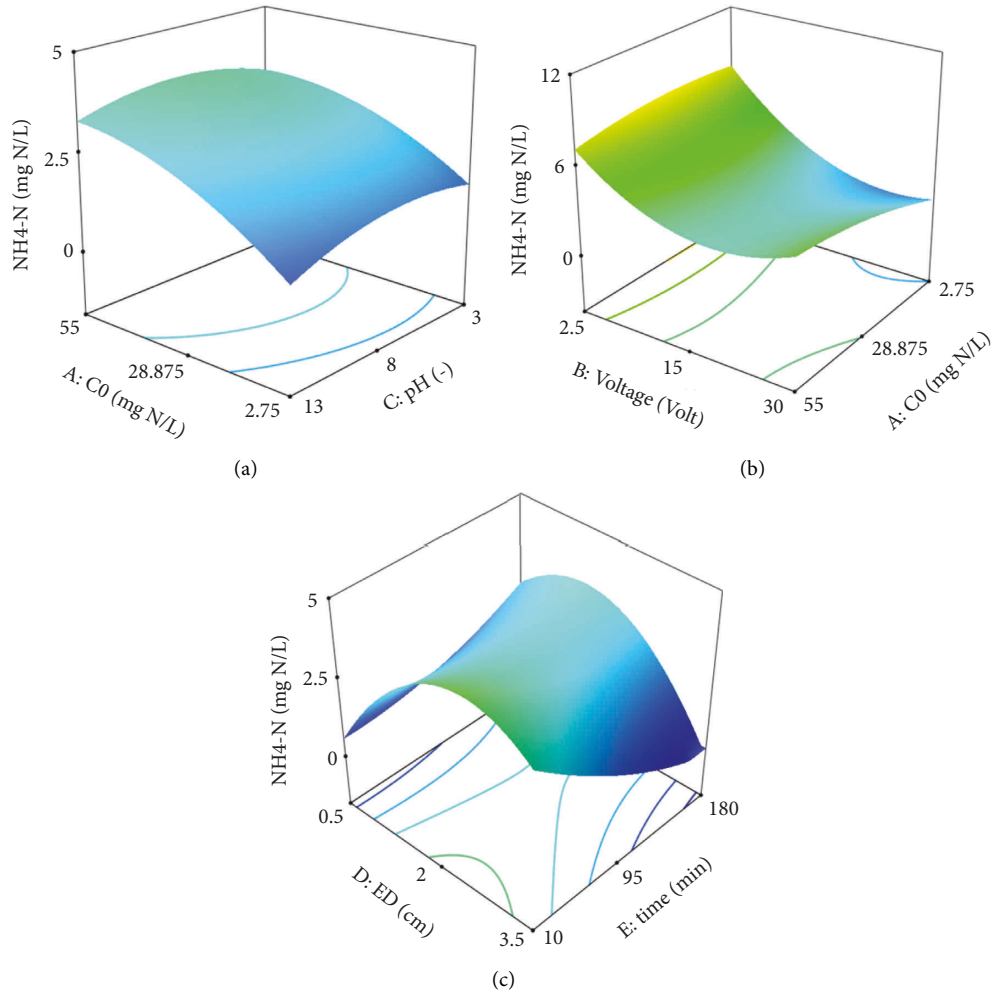

Figure 5: 3D surface plots for ammonia concentration.

lumps. The anode surface has a large number of cracks and pits after all experiments (Figure 6(a).B). The absence of lumps indicates wear in the material. Fe-SEM images of the cathode (graphite) at different resolutions show the change in morphology before and after EO process. Fresh electrode had homogeneous and uniform surface morphology all over (Figure 6(a).C), however, after the ECD process, it has pits, huge dents, and a nonuniform surface It looks as if many grains are scattered on the surface (Figure 6(a).D). By using FE-SEM, the surface of the electrodes can be observed to have changed due to wear of the electrodic material.

Figure 6(b).A and B show XRD patterns of fresh and used electrodes. The anode sheet (Ti/RuO_2) lost some crystallinity after the ECD process due to the decrease in peak intensities. The strongest metallic Ti/RuO_2 peak was at $2\theta = 40.01^{\circ}$, after which electrochemical denitrification had a sharp decline. $TiRuO_2$ peaks at angles of $2\theta = 76.00^{\circ}$, 77.50°, 82.50°, and 86.50 changed to Ti peaks as a result of RuO_2 reacting, some of the associated peaks have been removed. Figure 6(b).B shows the crystallography of the graphite cathode sheet. The strongest graphite peak at $2\theta = 26.5^{\circ}$ decreased significantly after the EO process (counts per second <10000). This change occurred due to nitrate ions adsorbing on the cathode sheet from the aqueous solution [3].

FTIR spectroscopy is used for the characterization of the functional groups in electrodes. As shown in Figure 6(c).A, there are no significant peaks in the FTIR spectrum of pristine graphite (before) that correspond to any functional groups. However, weak peaks are often observed that correspond to adsorbed water molecules. After ECD process, the peaks graphite FTIR spectrum at 1049 cm^{-1}, 1620 cm^{-1}, and 1581 cm^{-1} are assigned to the stretching vibration of C-O and C=O, respectively. The peak of–OH is broadened at 3421 cm^{-1}. The FTIR results indicate that the electrochemical oxidation increase the content of C-O groups and the number of -OH and C=O functional groups on the graphite surface. FTIR spectra of Ti/RuO_2 demonstrated to be reduced in the bands at 1214 cm^{-1} (C-O stretching), 2944 cm^{-1} (C-H stretching), and 3379 cm^{-1} (-OH) after electrochemical oxidation. The peak intensity of C=O (1654 cm−1) increases after the EO process (Figure 6(c).B).

3.6. Optimization and Sensitivity Analysis Using Monte Carlo Simulation and Energy Consumption. The statistical distributions implemented on the parameters using RStudio software are presented in Table 3. Then, 10,000 data were generated in statistical distributions. Following that, all

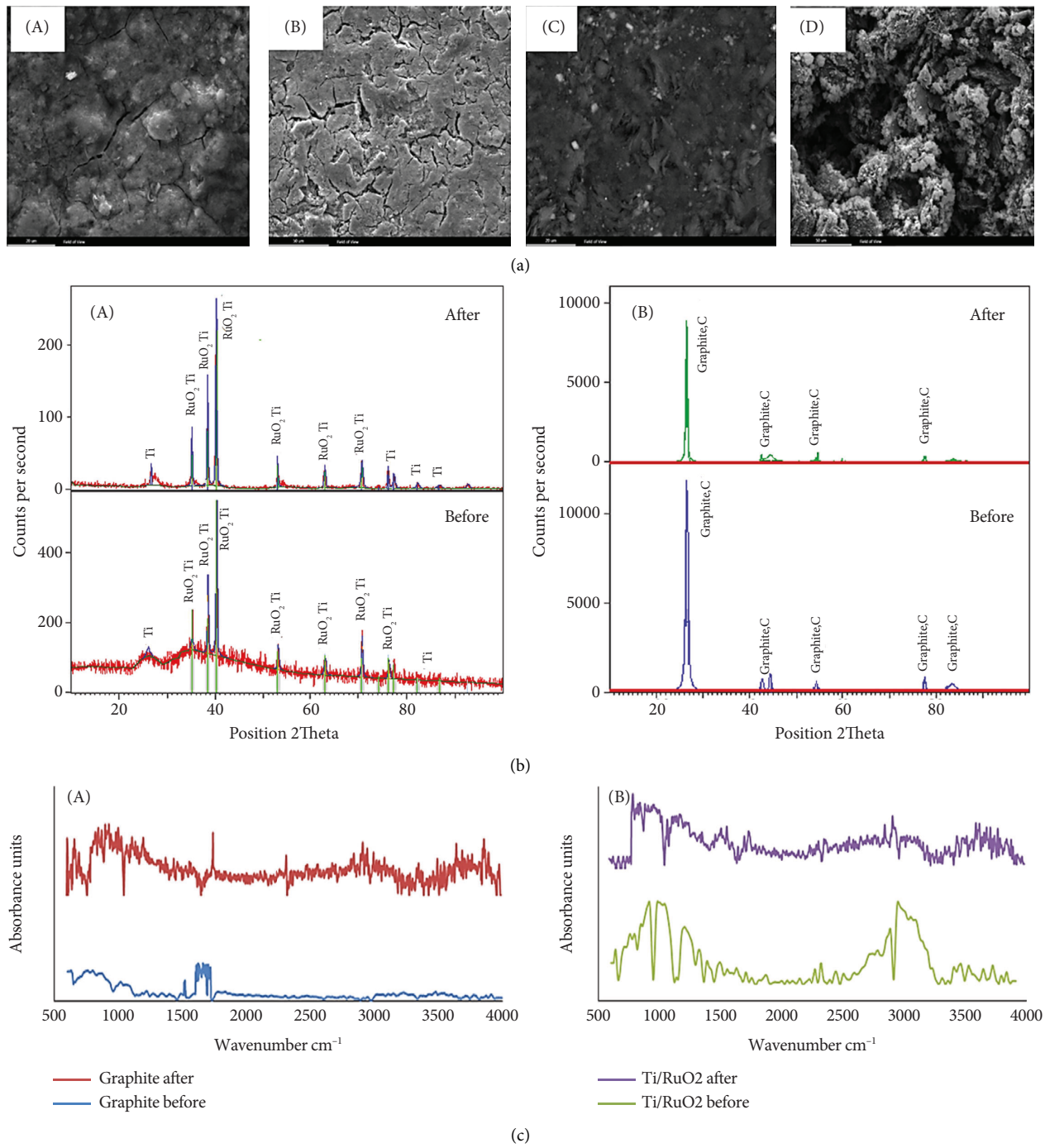

FIGURE 6: (a). SEM images of Ti/RuO_2 anode: (A) before; (B) after; and graphite cathode: (C) before; (D) after. (b) XRD pattern of (A) anode (Ti/RuO_2) and (B) cathode (graphite) for before and after. (c) FT-IR spectrums for (A) cathode (graphite) and (B) anode (Ti/RuO_2) for before and after of experiments.

generated data were placed in the output equation of the RSM model and the nitrate removal rate was determined. Five points with the highest removal rate in the results were selected and were experimented in the laboratory to specify the optimal point. The specified optimized conditions are the initial concentration of 30 ($mg\,L^{-1}$), voltage of 30 V, pH of 9.8, electrode distance of 0.7 cm, time of 90 min, and current density of about 2.9 mA/cm^2 (Table 5).

Then, sensitivity analysis was performed using spearman's rank correlation with the MCS approach. As shown in Figure 7, the most important parameters for nitrate removal are pH > ED > voltage > initial concentration > time, respectively. pH is considered a key factor of ECD performance in previous research works [3, 46, 49, 50]. The maximum spearman's rho of = 0.302 was for the pH. Electrode distance as the second effective parameter showed a negative correlation of (−0.246).

Table 5: Optimized conditions for nitrate removal in ECD process.

Variables	Unit	Optimized point
Initial concentration	mg N/L	30
Voltage	V	30
pH	—	9.8
ED	Cm	0.7
Time	Min	90
CD	mA/cm^2	2.9
Nitrate removal efficiency	%	98

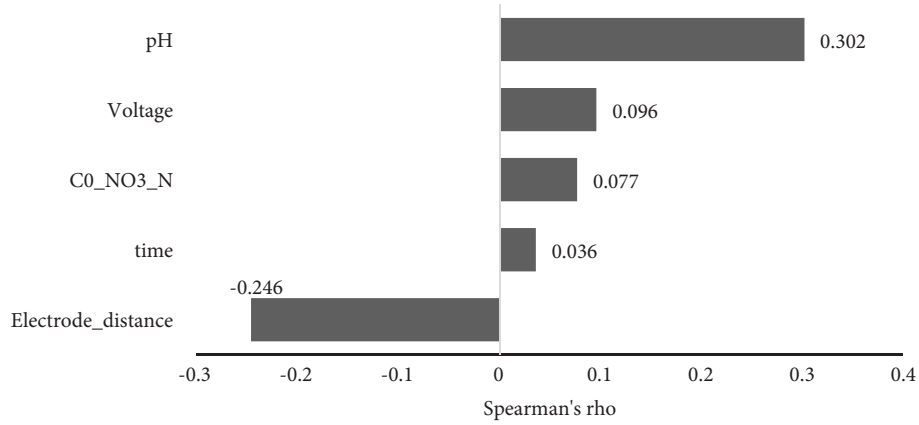

Figure 7: Sensitivity analysis using Spearman's rank correlation with MCS approach.

3.7. Current Density and Power Consumption at Optimum Point. Energy consumption and current efficiency parameters are used to compare the performance of electrochemical cells. Current efficiency is defined as the ratio of electrical current consumed to the total energy consumption. The term current efficiency involves both the mass transfer and the surface reactions in the system. Here, current efficiency and energy consumption are employed to represent the denitrification performance of electrochemical reactor in the optimum point [51, 52]. To calculate the mentioned parameters, the equations presented in the published articles were applied [53].

At the optimal point of the electrochemical denitrification reactor (mentioned in Section 3.6), the values of energy consumption and current efficiency were obtained as 389 kWh/kg NO_3^- and 84.49%, respectively.

3.8. Kinetics of Nitrate Removal in ECD Reactor. The experiments were performed at time intervals of 5, 15, 30, 60, and 90 min to achieve reaction kinetics in optimum conditions. The plots of three studied kinetic models included zero, first, and second order models, were presented in Figures 8(a)–8(c). According to the results, the second order kinetic model with R^2 equal to 0.93 was chosen as the best one for nitrate removal in the ECD reactor (Figure 8(c)). The plot of 1/[A] versus time for a second-order reaction is a straight line, with k = "slope of the line." The magnitude of k in this study was 0.367 $L \cdot mg^{-1} \cdot min^{-1}$. In previous kinetic studies, reactions related to the electrochemical removal of nitrate often followed first order [54, 55]. Chauhan et al. reported as the pH of the reactor increases, the reaction tends second order [3].

3.9. Investigation of Inorganic and Organic Compounds. As shown in Table 6, the addition of monovalent salt (NaCl), divalent salt ($ZnSO_4^-$), and glucose at concentrations of 1, 10, 100, and 1000 ($mg \cdot L^{-1}$), at the optimum point (i.e., $C_0 = 30$, PH = 9.8, voltage = 30 V, ED = 0.7 cm, and time = 90 min) decreases the nitrate removal rate, but it has increased the current density (CD). Of course, glucose has not changed the CD much. The best effect of monovalent and divalent salts on denitrification rate is at 100 $mg \cdot L^{-1}$ concentration. It also has a reducing effect at a concentration of 1000 $mg \cdot L^{-1}$. Chloride ions oxidized to hypochlorous acid and hypochlorite at the anode caused ammonia to be oxidized to nitrogen gas and nitrate. Furthermore, the presence of chloride ions inhibits the cathodic reduction of nitrate, thus causing to increasing denitrification rate [56]. The presence of glucose has led to a decrease of denitrification rate compared to its absence in the ECD reactor. Carry et al. demonstrated that injecting an organic carbon source (glucose) was the effective method to remove NO_3^- from water provided the biomass was available, while different doses of glucose without the biomass available had a decreasing effect on nitrate removal efficiency and denitrification rate [57]. Therefore, based on our results, it is assumed that the chemical mediators adsorbed on the anode surface due to electrochemical oxidation of glucose and so inhibit denitrification.

3.10. Nitrate Removal of Actual Samples by ECD Reactor. According to the results of the electrochemical oxidation process of three samples of groundwater wells (Table 7) at the optimum point (pH: 9.8, voltage: 0.35 V/cm^2, ED: 0.7 cm, time: 90 min (with increasing TDS from 394 to 1230 ($mg \cdot L^{-1}$), the nitrate removal efficiency decreased from 0.51

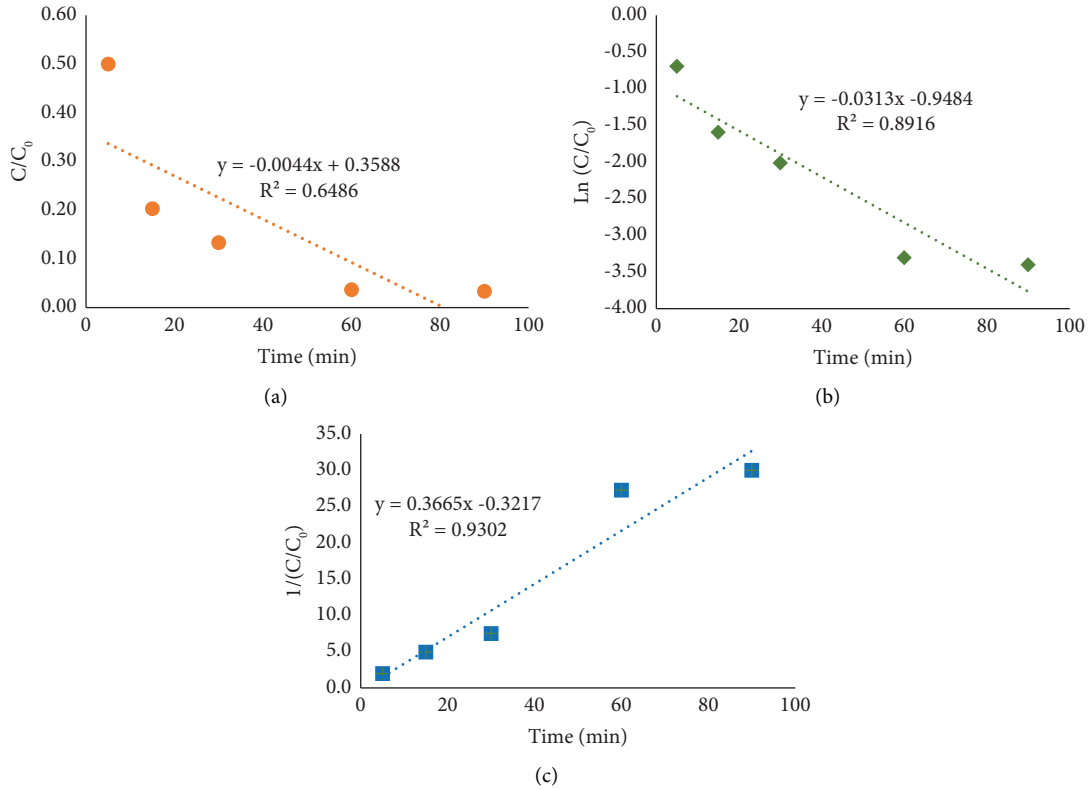

Figure 8: Kinetics plots of the three studied kinetic models: (a) zero order, (b) first order, and (c) second order.

Table 6: Performance of ECD reactor with addition of inorganic and organic compounds.

NaCl concentration (mg/L)	CD (mA/cm^2)	Nitrate removal rate	Denitrification rate
0	2.96	0.98	0.77
1	3.20	0.89	0.70
10	5.40	0.88	0.80
100	8.32	0.9	0.87
1000	8.32	0.78	0.76
$ZnSO_4$ concentration (mg/L)	CD (mA/cm^2)	Nitrate removal rate	Denitrification rate
0	2.96	0.98	0.77
1	3.19	0.84	0.74
10	3.02	0.86	0.80
100	7.58	0.88	0.86
1000	8.21	0.82	0.78
Glucose concentration (mg/L)	*CD (mA/cm^2)*	*Nitrate removal rate*	*Denitrification rate*
0	2.96	0.98	0.77
1	2.86	0.85	0.66
10	3.21	0.83	0.71
100	2.98	0.82	0.68
1000	2.96	0.81	0.43

Table 7: Well samples results.

Parameters	Unit	Well 1	Well 2	Well 3
TDS	mg/L	394.00	570.00	1230.00
NO_3-N in	mg/L	4.70	3.70	10.31
NO_2-N in	mg/L	0.01	0.01	0.06
NH_4-N in	mg/L	1.00	0.96	3.90
CD	mA/cm^2	8.00	8.00	8.00
Nitrate removal	%	51.06	37.84	34.04
Denitrification rate	%	50.73	28.31	33.12

to 0.34. In addition, increasing the TDS also reduced the denitrification rate. It seems that the ECD reactor has acceptable performance for real samples.

4. Conclusion

This study reports the electrochemical oxidation of nitrate from synthetic aqueous solutions with Ti/RuO_2 anode and graphite cathode electrodes. 47 experiments were designed with the CCD

method, and then the optimal point of the process was determined using the RSM model and its combination with the MCS. Nitrate removal efficiency of 98% was obtained at optimum conditions ($C_0 = 30$, PH = 9.8, voltage = 30 V, ED = 0.7 cm, and time = 90 min). FE-SEM, FTIR, and XRD techniques were used to characterize electrodes before and after all ECD experiments. Using the data generated by the MCS, sensitivity analysis was performed through the Spearman's rank correlation coefficient method. The parameters more affecting the nitrate removal efficiency were pH, ED, voltage, initial concentration, and time. The kinetics of the nitrate removal in the ECD reactor followed the second order with R^2 equal to 0.93. The magnitude of k in this study was $0.367 \cdot L \cdot mg^{-1} \cdot min^{-1}$. The addition of monovalent salt (NaCl), divalent salt ($ZnSO_4^-$), and glucose decreases the nitrate removal rate. The inorganic salts have increased the current density but the glucose has not changed it. The best effect of monovalent and divalent salts on denitrification rate is at 100 $mg \cdot L^{-1}$ concentration. The presence of glucose has led to a decrease in denitrification rate. In real well samples, the nitrate removal rate decreased from 0.51 to 0.34 and increasing the TDS reduced the denitrification rate. At the optimal point of the ECD reactor, the values of energy consumption and current efficiency were obtained as 389 kWh/kg NO_3^- and 84.49%, respectively.

Data Availability

All the data analyzed during this study are included in the article.

Conflicts of Interest

The authors declare that they have no conflicts of interest.

Acknowledgments

This article is the result of a M.Sc. thesis, No. 399234, which was conducted with the financial support of the Student Research Committee, School of Health, Isfahan University of Medical Sciences, Isfahan, Iran, with the ethics code IR.MUI.RESEARCH.REC.1399.307.

References

[1] S. Garcia-Segura, M. Lanzarini-Lopes, K. Hristovski, and P. Westerhoff, "Electrocatalytic reduction of nitrate: fundamentals to full-scale water treatment applications," *Applied Catalysis B: Environmental*, vol. 236, pp. 546–568, 2018.

[2] P. J. Thorburn, J. S. Biggs, K. L. Weier, and B. A. Keating, "Nitrate in groundwaters of intensive agricultural areas in coastal Northeastern Australia," *Agriculture, Ecosystems and Environment*, vol. 94, no. 1, pp. 49–58, 2003.

[3] R. Chauhan and V. C. Srivastava, "Electrochemical denitrification of highly contaminated actual nitrate wastewater by Ti/RuO2 anode and iron cathode," *Chemical Engineering Journal*, vol. 386, Article ID 122065, 2020.

[4] Z. shamsizadeh, M. H. Ehrampoush, M. Nikaeen et al., "Antibiotic resistance and class 1 integron genes distribution in irrigation water-soil-crop continuum as a function of irrigation water sources," *Environmental Pollution*, vol. 289, Article ID 117930, 2021.

[5] J. Lakshmi, G. Sozhan, and S. Vasudevan, "Recovery of hydrogen and removal of nitrate from water by electrocoagulation process," *Environmental Science & Pollution Research*, vol. 20, no. 4, pp. 2184–2192, 2013.

[6] J. F. Su, I. Ruzybayev, I. Shah, and C. P. Huang, "The electrochemical reduction of nitrate over micro-architectured metal electrodes with stainless steel scaffold," *Applied Catalysis B: Environmental*, vol. 180, pp. 199–209, 2016.

[7] C. Della Rocca, V. Belgiorno, and S. Meriç, "Overview of in-situ applicable nitrate removal processes," *Desalination*, vol. 204, pp. 46–62, 2007.

[8] M. Shrimali and K. P. Singh, "New methods of nitrate removal from water," *Environmental Pollution*, vol. 112, no. 3, pp. 351–359, 2001.

[9] B. P. Dash and S. Chaudhari, "Electrochemical denitrificaton of simulated ground water," *Water Research*, vol. 39, no. 17, pp. 4065–4072, 2005.

[10] B. U. Bae, Y. H. Jung, W. W. Han, and H. S. Shin, "Improved brine recycling during nitrate removal using ion exchange," *Water Research*, vol. 36, no. 13, pp. 3330–3340, 2002.

[11] "1991 nature publishing group grachel," *Nature*, vol. 353, pp. 412–414, 1991.

[12] L. Su, K. Li, H. Zhang et al., "Electrochemical nitrate reduction by using a novel Co3O4/Ti cathode," *Water Research*, vol. 120, 2017.

[13] Z. Shen, D. Wu, J. Yang, T. Yuan, W. H. Wang, and J. P. Jia, "Methods to improve electrochemical treatment effect of dye wastewater," *Journal of Hazardous Materials*, vol. 131, 2006.

[14] L. Chiang, J. Chang, and T.-C. Wen, "Indirect oxidation effect in electrochemical oxidation treatment of landfill leachate," *Water Reasearch*, vol. 29, 1995.

[15] Ş. İrdemez, N. Demircioğlu, Y. Yıldız, and Z. Bingül, "The effects of current density and phosphate concentration on phosphate removal from wastewater by electrocoagulation using aluminum and iron plate electrodes," *Separation and Purification Technology*, vol. 52, pp. 218–223, 2006.

[16] N. Kumar and V. C. Srivastava, "Simple synthesis of large graphene oxide sheets via electrochemical method coupled with oxidation process," *ACS Omega*, vol. 3, no. 8, pp. 10233–10242, 2018.

[17] G. Dima, A. De Vooys, and M. T. M Kooper, "Electrocatalytic reduction of nitrate at low concentration on coinage and transition-metal electrodes in acid solutions," *Journal of Electroanalytical Chemistry*, vol. 554-555, 2003.

[18] M. Kalaruban, P. Loganathan, J. Kandasmy, R. Naidu, and S. Vigneshwaran, "Enhanced removal of nitrate in an integrated electrochemical-adsorption system," *Separation and Purification Technology*, vol. 189, 2017.

[19] E. Lacasa, P. Canizares, and J. Llanos, "Effect of the cathode material on the removal of nitrates by electrolysis in non-chloride media," *Journal of Hazardous Materials*, pp. 213-214, 2012, https://www.sciencedirect.com/science/article/abs/pii/S0304389412001914.

[20] W. Y. Kim, D.-J. Son, C.-Y. Yun et al., "Performance assessment of electrolysis using copper and catalyzed electrodes for enhanced nutrient removal from wastewater," *Journal of Electrochemical Science and Technology*, vol. 8, 2017.

[21] J. Sim, H. Seo, and J. Kim, "Electrochemical denitrification of metal-finishing wastewater: influence of operational parameters," *Korean Journal of Chemical Engineering*, vol. 29, no. 4, pp. 483–488, 2012.

[22] J. O. Bockris and J. Kim, "Electrochemical reductions of Hg(II), ruthenium-nitrosyl complex, chromate, and nitrate in

a strong alkaline solution," *Journal of the Electrochemical Society*, vol. 143, no. 12, pp. 3801–3808, 1996.

[23] A. De Vooys, R. A. van Santen, and J. A. R. van Veen, "Electrocatalytic reduction of NO3− on palladium/copper electrodes," *Journal of Molecular Catalysis A: Chemical*, vol. 154, 2000.

[24] W. Li, C. Xiao, Y. Zhao, Q. Zhao, R. Fan, and J. Xue, "Electrochemical reduction of high-concentrated nitrate using Ti/TiO2 nanotube Array anode and Fe cathode in dual-chamber cell," *Catalysis Letters*, vol. 146, no. 12, pp. 2585–2595, 2016.

[25] A. Ansari and D. Nematollahi, "Convergent paired electrocatalytic degradation of p-dinitrobenzene by Ti/SnO2-Sb/β-PbO2 anode. A new insight into the electrochemical degradation mechanism," *Applied Catalysis B: Environmental*, vol. 261, no. August 2019, Article ID 118226, 2020.

[26] Z. Merati and J. Basiri Parsa, "Enhancement of the catalytic activity of Pt nanoparticles toward methanol electro-oxidation using doped-SnO2 supporting materials," *Applied Surface Science*, vol. 435, pp. 535–542, 2018.

[27] Q. Fu, L. C. Colmenares Rausseo, U. Martinez et al., "Effect of Sb segregation on conductance and catalytic activity at Pt/Sb-doped SnO2 interface: a synergetic computational and experimental study," *ACS Applied Materials and Interfaces*, vol. 7, no. 50, pp. 27782–27795, 2015.

[28] Y. Zeng, C. Priest, G. Wang, and G. Wu, "Restoring the nitrogen cycle by electrochemical reduction of nitrate: progress and prospects," *Small Methods*, vol. 4, no. 12, pp. 1–28, 2020.

[29] M. Hasanpour, S. Motahari, D. Jing, and M. Hatami, "Statistical analysis and optimization of photodegradation efficiency of methyl orange from aqueous solution using cellulose/zinc oxide hybrid aerogel by response surface methodology (RSM)," *Arabian Journal of Chemistry*, vol. 14, no. 11, Article ID 103401, 2021.

[30] M. Ghazouani, H. Akrout, and L. Bousselmi, "Nitrate and carbon matter removals from real effluents using Si/BDD electrode," *Environmental Science and Pollution Research*, vol. 24, pp. 9895–9906, 2017.

[31] Y. H. Liou, C. J. Lin, S. C. Weng, H. H. Ou, and S. L. Lo, "Selective decomposition of aqueous nitrate into nitrogen using iron deposited bimetals," *Environmental Science and Technology*, vol. 43, no. 7, pp. 2482–2488, 2009.

[32] W. Zhao, X. Zhu, Y. Wang, Z. Ai, and D. Zhao, "Catalytic reduction of aqueous nitrates by metal supported catalysts on Al particles," *Chemical Engineering Journal*, vol. 254, pp. 410–417, 2014.

[33] A. A. Babaei, R. R. Kalantary, A. Azari, and B. Kakavandi, "Enhanced removal of nitrate from water using nZVI@ MWCNTs composite: synthesis, kinetics and mechanism of reduction," *Water Science and Technology*, vol. 72, no. 11, pp. 1988–1999, 2015.

[34] M. Li, C. Feng, Z. Zhang et al., "Simultaneous reduction of nitrate and oxidation of by-products using electrochemical method," *Journal of Hazardous Materials*, vol. 171, no. 1–3, pp. 724–730, 2009.

[35] K. Wada, T. Hirata, S. Hosokawa, S. Iwamoto, and M. Inoue, "Effect of supports on Pd-Cu bimetallic catalysts for nitrate and nitrite reduction in water," *Catalysis Today*, vol. 185, no. 1, pp. 81–87, 2012.

[36] A. Kumar, A. Rana, C. Guo et al., "Acceleration of photo-reduction and oxidation capabilities of Bi4O5I2/SPION@ calcium alginate by metallic Ag: wide spectral removal of nitrate and azithromycin," *Chemical Engineering Journal*, vol. 423, Article ID 130173, 2021.

[37] W. E. Federation, "Standard methods for the examination of water and wastewater standard methods for the examination of water and wastewater," *Public Health*, vol. 51, no. 1, p. 940, 1999.

[38] G. Mannina, A. Cosenza, G. Viviani, and G. A. Ekama, "Sensitivity and uncertainty analysis of an integrated ASM2d MBR model for wastewater treatment," *Chemical Engineering Journal*, vol. 351, pp. 579–588, 2018.

[39] M. M. Emamjomeh, H. A. Jamali, and M. Moradnia, "Optimization of nitrate removal efficiency and energy consumption using a batch monopolar electrocoagulation: prediction by RSM method," *Journal of Environment and Engineering*, vol. 143, no. 7, Article ID 04017022, 2017.

[40] B. Bina, F. Mohammadi, M. M. Amin, H. R. Pourzamani, and Z. Yavari, "Evaluation of the effects of AlkylPhenolic compounds on kinetic coefficients and biomass activity in MBBR by means of respirometric techniques," *Chinese Journal of Chemical Engineering*, vol. 26, no. 4, pp. 822–829, 2018.

[41] B. A. Abdulhadi, P. Kot, K. S. Hashim, A. Shaw, and R. A. Khaddar, "Influence of current density and electrodes spacing on reactive red 120 dye removal from dyed water using electrocoagulation/electroflotation (EC/EF) process," *IOP Conference Series: Materials Science and Engineering*, vol. 584, no. 1, Article ID 012035, 2019.

[42] V. Khandegar and A. K. Saroha, "Electrocoagulation for the treatment of textile industry effluent - a review," *Journal of Environmental Management*, vol. 128, pp. 949–963, 2013.

[43] M. S. Kothari and K. A. Shah, "Electrochemical oxidation for decolorization of Rhodamine-B dye using mixed metal oxide electrode: modeling and optimization," *Water Science Technology*, vol. 81, pp. 720–731, 2020.

[44] Z. Souri, A. Ansari, D. Nematollahi, and M. Mazloum-Ardakani, "Electrocatalytic degradation of dibenzoazepine drugs by fluorine doped β-PbO2 electrode: new insight into the electrochemical oxidation and mineralization mechanisms," *Journal of Electroanalytical Chemistry*, vol. 862, Article ID 114037, 2020.

[45] A. Ansari and D. Nematollahi, "A comprehensive study on the electrocatalytic degradation, electrochemical behavior and degradation mechanism of malachite green using electrodeposited nanostructured β-PbO2 electrodes," *Water Research*, vol. 144, pp. 462–473, 2018.

[46] A. K. Benekos, M. Tsigara, S. Zacharakis et al., "Combined electrocoagulation and electrochemical oxidation treatment for groundwater denitrification," *Journal of Environmental Management*, vol. 285, no. January, Article ID 112068, 2021.

[47] K. S. Hashim, A. Shaw, R. Al Khaddar, M. O. Pedrola, and D. Phipps, "Energy efficient electrocoagulation using a new flow column reactor to remove nitrate from drinking water––experimental, statistical, and economic approach," *Journal of Environmental Management*, vol. 196, pp. 224–233, 2017.

[48] R. S. Jasna, R. Gandhimathi, A. Lavanya, and S. T. Ramesh, "An integrated electrochemical-Adsorption system for removal of nitrate from water," *Journal of Environmental Chemical Engineering*, vol. 8, no. 5, Article ID 104387, 2020.

[49] M. Malakootian, N. Yousefi, and A. Fatehizadeh, "Survey efficiency of electrocoagulation on nitrate removal from aqueous solution," *International journal of Environmental Science and Technology*, vol. 8, no. 1, pp. 107–114, 2011.

[50] S. Kumar, S. Singh, and V. C. Srivastava, "Electro-oxidation of nitrophenol by ruthenium oxide coated titanium electrode:

parametric, kinetic and mechanistic study," *Chemical Engineering Journal*, vol. 263, pp. 135–143, 2015.

[51] M. R. Samarghandi, A. Ansari, A. Dargahi et al., "Enhanced electrocatalytic degradation of bisphenol A by graphite/β-PbO2 anode in a three-dimensional electrochemical reactor," *Journal of Environmental Chemical Engineering*, vol. 9, no. 5, Article ID 106072, 2021 Oct 1.

[52] M. R. Samarghandi, A. Dargahi, A. Rahmani, A. Shabanloo, A. Ansari, and D. Nematollahi, "Application of a fluidized three-dimensional electrochemical reactor with Ti/SnO2–Sb/β-PbO2 anode and granular activated carbon particles for degradation and mineralization of 2, 4-dichlorophenol: process optimization and degradation pathway," *Chemosphere*, vol. 279, Article ID 130640, 2021.

[53] J. Rodziewicz, A. Mielcarek, W. Janczukowicz, and K. Bryszewski, "Electric power consumption and current efficiency of electrochemical and electrobiological rotating disk contactors removing nutrients from waste water generated in soil-less plant cultivation systems," *Water (Switzerland)*, vol. 12, no. 1, pp. 213–223, 2020.

[54] M. Li, C. Feng, Z. Zhang, S. Yang, and N. Sugiura, "Treatment of nitrate contaminated water using an electrochemical method," *Bioresource Technology*, vol. 101, no. 16, pp. 6553–6557, 2010.

[55] G. Pérez, R. Ibáñez, A. M. Urtiaga, and I. Ortiz, "Kinetic study of the simultaneous electrochemical removal of aqueous nitrogen compounds using BDD electrodes," *Chemical Engineering Journal*, vol. 197, pp. 475–482, 2012.

[56] Q. Song, M. Li, L. Wang, X. Ma, F. Liu, and X. S. C. Liu, "Mechanism and optimization of electrochemical system for simultaneous removal of nitrate and ammonia," *Journal of Hazardous Materials*, vol. 363, pp. 119–126, 2019.

[57] R. Carrey, N. Otero, G. Vidal-Gavilan, C. Ayora, A. Soler, and J. J. Gómez-Alday, "Induced nitrate attenuation by glucose in groundwater: flow-through experiment," *Chemical Geology*, vol. 370, no. 2, pp. 19–28, 2014.